Leading-order calculation of hadronic contributions to the Muon *g*-2 using the Dyson–Schwinger approach

Tobias Goecke [a], Christian S. Fischer [a,b,*], Richard Williams [c]

[a] *Institut für Theoretische Physik, Universität Giessen, 35392 Giessen, Germany*
[b] *Gesellschaft für Schwerionenforschung mbH, Planckstr. 1, D-64291 Darmstadt, Germany*
[c] *Dept. Física Teoríca I, Universidad Complutense, 28040 Madrid, Spain*

A B S T R A C T

We present a calculation of the hadronic vacuum polarisation (HVP) tensor within the framework of Dyson–Schwinger equations. To this end we use a well-established phenomenological model for the quark–gluon interaction with parameters fixed to reproduce hadronic observables. From the HVP tensor we compute both the Adler function and the HVP contribution to the anomalous magnetic moment of the muon, a_μ. We find $a_\mu^{\mathrm{HVP}} = 6760 \times 10^{-11}$ which deviates about two percent from the value extracted from experiment. Additionally, we make comparison with a recent lattice determination of a_μ^{HVP} and find good agreement within our approach. We also discuss the implications of our result for a corresponding calculation of the hadronic light-by-light scattering contribution to a_μ.

© 2011 Elsevier B.V. Open access under CC BY license.

1. Introduction

One of the most interesting places to search for new physics beyond the Standard Model (SM) is the anomalous magnetic moment of the muon, a_μ. It is dominated by QED effects, however due to the heavy mass of the muon it is also sensitive to other corrections. Aside from weak interaction contributions which can be evaluated in perturbation theory, one also has to include effects from QCD. Since the latter are intrinsically non-perturbative at the scales relevant to the calculation, they are much harder to include systematically.

Experimental efforts at Brookhaven National Lab and elaborated theoretical efforts of the past ten years have pinned down a_μ to the 10^{-11} level, leading to significant deviations between theory [1] and experiment [2,3]:

Experiment: $116\,592\,089.0(63.0) \times 10^{-11}$,   (1)

Theory: $116\,591\,790.0(64.6) \times 10^{-11}$.   (2)

This 3.3σ deviation might be seen as a sign for new physics, however confirmation requires that the uncertainties of both theory and experiment must be reduced yet further. The error on the theoretical side is dominated by hadronic contributions involving non-perturbative QCD dynamics. The leading-order hadronic
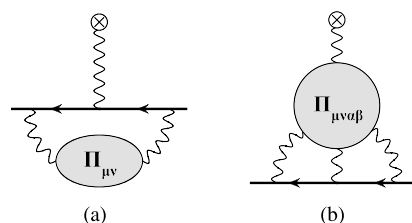

Fig. 1. The two classifications of corrections to the photon–muon vertex function: (a) hadronic vacuum polarisation contribution to a_μ. The vertex is dressed by the vacuum polarisation tensor $\Pi_{\mu\nu}$; (b) the hadronic light-by-light scattering contribution to a_μ.

contribution is the hadronic vacuum polarisation insertion (HVP) shown in Fig. 1(a). At present, this diagram also dominates the theoretical error of a_μ from the SM. One obtains [4]

$$a_\mu^{(\mathrm{HVP})} = \left[6\,903.0(52.6) - 100.3(1.1) \right] \times 10^{-11}, \quad (3)$$

for the leading and subleading contributions, see also Refs. [5,6] for recent updates. The HVP-tensor ($\Pi_{\mu\nu}$) involved in the calculation of the leading-order result can be obtained from experimental input by recourse to the optical theorem; such results can then be regarded as being model independent. However, note that models may be involved in the analysis or extraction of this experimental data, especially in the (dominant) low Q^2 region [7].

The diagram that, in the literature, yields the second largest theoretical error is that of hadronic light-by-light scattering (LBL), Fig. 1(b). It is extremely difficult to measure and therefore needs

* Corresponding author at: Institut für Theoretische Physik, Universität Giessen, 35392 Giessen, Germany.

E-mail address: christian.fischer@theo.physik.uni-giessen.de (C.S. Fischer).

to be determined from theory alone. There is a long history of different approaches to this problem, see Ref. [1] for an overview. Recently, we provided a re-evaluation of a_μ^{LBL} in the framework of Dyson–Schwinger and Bethe–Salpeter equations of QCD [8,9]. Starting with a phenomenologically successful model for the quark–gluon interaction, we determined dynamically the momentum dependent quark propagator, the corresponding meson Bethe–Salpeter amplitudes and the quark–photon vertex and used these as building blocks for our calculation of a_μ^{LBL}. In contrast to previous approaches, we automatically included effects in the quark–photon interaction that are induced by gauge invariance. This can be seen as one of the improvements that DSEs have over typical effective approaches to QCD. Our results indicate that the theoretical value of Eq. (2) may indeed receive additional positive contributions that reduce the discrepancy with experiment. The precise size of these contributions, however, will only become clear once we reduce the approximations made in [8,9].

While work in this direction is in progress, we find it prudent to elucidate upon and justify our approach via a calculation of the hadronic vacuum polarisation $\Pi_{\mu\nu}$. Although this quantity in principle need not be determined from theory for the purposes of a_μ, it serves as an important testing ground for any approach used for calculating hadronic contributions to a_μ [10–14]. In this Letter we provide results for the HVP contribution to the muon anomaly together with the Adler function. We employ the same model and philosophy as used recently in our calculation of hadronic light-by-light scattering [8,9]. By comparing to the results extracted from experiment and to recent lattice calculations [15] we will demonstrate that our approach provides meaningful and quantitatively reliable results. We also believe that our results serve to address and invalidate an argument made by the authors of Ref. [16]. There, one-loop radiative corrections to a_μ^{HVP} and a_μ^{LBL} in a constituent quark model have been invoked to argue against large effects from vertex corrections. While their calculation is no doubt correct – within the limitations of using perturbation theory at strong coupling scales – the relevance of their results to the case of g-2 seems rather limited. This will be discussed in more detail below.

The outline of the Letter is as follows. In Section 2 we will introduce the hadronic vacuum polarisation, starting with its basic definition and its calculation within the functional approach. In Section 3 we present the framework that we employ in this Letter, the Dyson–Schwinger (DSE) and Bethe–Salpeter (BSE) equations. This is followed by our results and a discussion pertaining a_μ^{HVP} and the Adler function in Section 4. Finally we summarise and discuss the relevance of our results for a_μ^{LBL} in the concluding sections.

2. The hadronic vacuum polarisation contribution

In the following we give the basic definitions concerning the HVP tensor, the muon anomaly and the Adler function. Throughout this work we will employ Euclidean space conventions.

2.1. Basic definitions

The hadronic vacuum polarisation tensor $\Pi_{\mu\nu}$ is defined as that part of the one particle irreducible (1PI) photon self-energy that is generated by QCD dynamics. It can be obtained from the photon Dyson–Schwinger equation

$$D_{\mu\nu}^{-1}(q) = Z_3 \big(D_{\mu\nu}^{(0)}(q)\big)^{-1} - e^2 \Pi_{\mu\nu}(q), \tag{4}$$

where $D_{\mu\nu}$ is the full photon propagator, $D_{\mu\nu}^{(0)}$ the bare propagator and Z_3 is the photon renormalisation constant. The hadronic
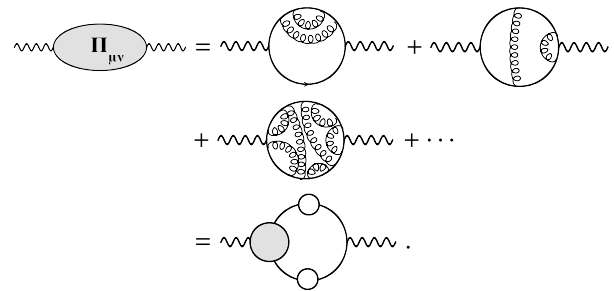

Fig. 2. The photon vacuum polarisation and its expansion in planar diagrams.

tensor $\Pi_{\mu\nu}$, specified explicitly below, can also be seen as the 1PI-part of the current correlator

$$\Pi_{\mu\nu}(q) = \int_x e^{iq\cdot x} \langle j_\mu(x) j_\nu(0) \rangle_{1PI,hadr.}, \tag{5}$$

with $\int_x = \int d^4x$ and the electromagnetic quark current j_μ given by

$$j_\mu = \frac{2}{3}\bar{u}\gamma_\mu u - \frac{1}{3}\bar{d}\gamma_\mu d - \frac{1}{3}\bar{s}\gamma_\mu s + \frac{2}{3}\bar{c}\gamma_\mu c - \frac{1}{3}\bar{b}\gamma_\mu b. \tag{6}$$

Here u, d, s, c and b are the respective quark spinors. It follows from the Ward–Takahashi identity (WTI) $q_\mu \Pi_{\mu\nu} = 0$ that the HVP tensor is transverse:

$$\Pi_{\mu\nu}(q) = \left(\delta_{\mu\nu} - \frac{q_\mu q_\nu}{q^2}\right)q^2 \Pi(q^2), \tag{7}$$

which serves as a definition of the scalar vacuum polarisation $\Pi(q^2)$. The quantity $\Pi(q^2)$ is logarithmically divergent and has to be renormalised. We choose the condition $\Pi(0) = 0$ which leaves the definition of the electric charge intact. More details concerning our renormalisation prescription can be found below.

Once we have obtained the renormalised HVP scalar, $\Pi_R(q^2)$, the leading hadronic contribution to a_μ^{HVP} can be calculated [10]

$$a_\mu^{HVP} = \frac{\alpha}{\pi} \int_0^1 dx\,(1-x)\left[-e^2 \Pi_R\left(\frac{x^2}{1-x}m_\mu^2\right)\right], \tag{8}$$

where m_μ is the muon mass and $\alpha = e^2/4\pi$ is the fine structure constant.

The Adler function $D(q)$ is defined as the logarithmic derivative of the polarisation scalar

$$D(q) = -q^2 \frac{d\Pi(q^2)}{dq^2}. \tag{9}$$

The HVP tensor and the Adler function can be obtained independently of the model from experiment, exploiting dispersion relations (see e.g. [1,4] for details).

2.2. Expansion in a functional approach

In a functional approach the vacuum polarisation tensor is essentially the photon self-energy. For hadronic contributions these photons couple to quarks, which in turn couple to gluons. It thus contains a resummation of an infinity of diagrams. In the spirit of the $1/N_c$ counting we consider only those diagrams which are planar. This infinite subset of diagrams is the same as those considered in [8,9]. The resulting expansion is depicted graphically in Fig. 2. The first diagram on the right hand side shows gluonic corrections that non-perturbatively dress the current quark. The second diagram shows gluonic corrections to the quark–photon
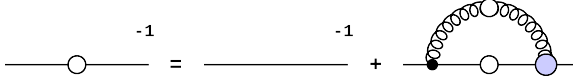
Fig. 3. Dyson–Schwinger equation for the quark propagator. Specification of the fully-dressed gluon propagator (wiggly line) and quark–gluon vertex (grey blob) define the truncation scheme.

vertex. Both classes of diagrams are indicated in the third diagram, showing the complexity of the resummation. These are finally written in terms of fully-dressed one-particle irreducible Green's functions (propagators and vertices marked by circles) in the second line of the equation. These are calculated self-consistently within a rainbow-ladder approximation to their DSEs, detailed in the next section. Note that the diagram in the last line of Fig. 2 is an exact representation of the hadronic tensor. The truncation takes place on the level of the propagator and the vertex.

3. Framework

In the following we summarise the calculation scheme employed in this Letter; more explicit details can be found in Ref. [9]. The Dyson–Schwinger equations (DSEs) are exact relations amongst the Green's function of a given theory. Since they constitute an infinite tower of coupled integral equations a truncation has to be employed to provide tractability. For the calculation of the Adler function and the muon anomaly, we need the quark propagator, quark–photon vertex and hadronic vacuum polarisation tensor. These are obtained from their respective DSEs, which we detail below.

3.1. The quark DSE

We begin with the dressed quark propagator $S(p)$,

$$S(p) = Z_f(p^2)\left(i\not{p} + M(p^2)\right)^{-1}, \tag{10}$$

which is characterised by the momentum dependent quark mass function $M(p^2)$ and the wave function $Z_f(p^2)$. These are obtained as a solution of the quark DSE given diagrammatically in Fig. 3. On the right hand side the inverse bare quark propagator is given by $S^{-1}(p) = Z_2(i\not{p} + m)$ with quark renormalisation factor Z_2 and the bare mass m. The quark self-energy contains the gluon propagator, given in Landau gauge as

$$D_{\mu\nu}(k) = \left(\delta_{\mu\nu} - \frac{k_\mu k_\nu}{k^2}\right)\frac{Z(k^2)}{k^2}, \tag{11}$$

with dressing function $Z(k^2)$. In addition the dressed quark–gluon vertex $\Gamma_\mu(p,q)$ is required. A simple, yet phenomenologically successful approximation of the quark–gluon interaction has been suggested by Maris and Tandy [17]. Here only the leading Dirac structure of the vertex is retained $\Gamma_\mu(k^2) = \gamma_\mu \Gamma^{YM}(k^2)$ and the dressing of the Yang–Mills (YM) part of the vertex is chosen to depend on the gluon momentum k only. The combination of the gluon- and vertex-dressing functions is then modelled as

$$Z(k^2)\Gamma^{YM}(k^2) = \frac{4\pi}{g^2}\left(\frac{\pi}{\omega^6}Dk^4\exp\left(-k^2/\omega^2\right)\right.$$
$$\left. + \frac{2\pi\gamma_m}{\log(\tau + (1 + k^2/\Lambda_{QCD}^2)^2)}\left[1 - e^{-k^2/(4m_t^2)}\right]\right), \tag{12}$$

with $m_t = 0.5$ GeV, $\tau = e^2 - 1$, $\gamma_m = 12/(33 - 2N_f)$, $\Lambda_{QCD} = 0.234$ GeV, $\omega = 0.4$ GeV and $D = 0.93$ GeV². This model interaction assumes the form of the one-loop running coupling of QCD

Table 1
Two choices for the light bare quark masses at $\mu^2 = (19\ \text{GeV})^2$ and the resulting meson masses (in MeV) in the pseudoscalar and vector meson sector. For the heavy quarks we always take $m_c = 827$ MeV and $m_b = 3680$ MeV which lead to good results for charmonia and bottomonia in the pseudoscalar and vector channel.

	$m_{u,d}$ [MeV]	m_s [MeV]	m_π [MeV]	m_K [MeV]	$m_{\rho,\omega}$ [MeV]	m_ϕ [MeV]
Set I	3.7	85	138	495	740	1080
Set II	11	72	240	477	770	1020

at momenta $k^2 \gg \Lambda_{QCD}^2$ and provides enough interaction strength in the infrared for dynamical chiral symmetry breaking to occur. As for our regularisation procedure in order to precisely satisfy the Ward-identity for the fermion–photon vertex we work with a Pauli–Villars scheme. The resulting vertex and propagators satisfy the identity on the permille level.

Combining the DSE with the corresponding Bethe–Salpeter equation (BSE) one can determine mesonic bound state masses and their decay constants. Since our rainbow-ladder model satisfies the axial-vector Ward–Takahashi identity, these are related to the renormalised quark mass $m(\mu^2)$ and the quark condensate at our renormalisation point $\mu^2 = 19$ GeV² according to the Gell-Mann Oakes Renner relation. For details see e.g. Ref. [18,19]. The model parameters ω and D are then chosen such that the physical value of the pion decay constant is reproduced. The quark masses have then been fixed by comparison with experimental meson masses in the pseudoscalar meson sector, cf. the first set in Table 1. Together with the self-consistently calculated quark–photon vertex (see below) electromagnetic properties such as electromagnetic form factors and charge radii can be obtained [20,21] that are in good agreement with experiment. This is also true for heavy flavors as discussed in Ref. [22]. Especially important for the calculation of the HVP tensor is, however, the behaviour of the model in the vector meson channel. Here, the deviation to experiment is on the five percent level, as can be seen from the first line of Table 1. It is therefore not unreasonable to expect that the model provides a good description of hadronic contributions to $\Pi_{\mu\nu}$ up to potential deviations of the order of five to ten percent to the experimental value. One possibility to investigate the systematic error of the model further, is to fix the bare quark masses not with pseudoscalar meson masses, but with the vector meson sector. The corresponding values are given in the second line of Table 1. Naturally, such a change in parameters is at the expense of the pseudoscalar sector and we obtain a quite heavy pion. In a full treatment this would in turn affect the decay width of the ρ-meson. Since in our rainbow-ladder approach this decay is not taken into account anyway we can ignore this effect. Below, we will employ both mass parameter sets in our calculation of a_μ^{HVP} and estimate the model inherent systematic error by a comparison of the results.

3.2. The quark–photon vertex

The second ingredient necessary for the determination of the hadronic tensor through Fig. 2 is the fully-dressed quark–photon vertex. This quantity is obtained self-consistently from its inhomogeneous Bethe–Salpeter equation

$$\Gamma_\mu(P,k) = Z_2\gamma_\mu + \frac{4}{3}g^2 Z_2^2$$
$$\times \int_q \left[\gamma_\alpha S(q_-)\Gamma_\mu(P,q)S(q_+)\gamma_\beta\right]D_{\alpha\beta}(r^2)\Gamma^{YM}(r^2), \tag{13}$$
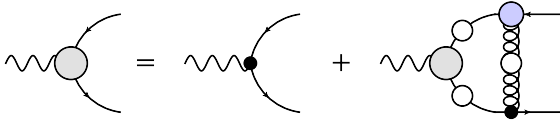
Fig. 4. Inhomogeneous BSE for the quark–photon vertex.

where $r = q - k$ and $\int_q = \int \frac{d^4q}{(2\pi)^4}$. We show the BSE pictorially in Fig. 4. Again we use the ladder truncation ensuring that both the axial-vector and vector Ward–Takahashi identities (WTIs) are satisfied. To this end the quark–gluon interaction in (13) needs to be the same as the one in the quark DSE.

In general, the quark–photon vertex can be decomposed into twelve covariants

$$\Gamma_\mu(P, k) = \sum_{i}^{12} V_\mu^{(i)} \lambda^{(i)}(P, k), \qquad (14)$$

where V_μ are the covariant tensor structures and $\lambda^{(i)}(P, k)$ are non-trivial scalar dressing functions that contain the non-perturbative dynamics. The photon momentum is P, with k the relative quark momentum such that the incoming and outgoing quark momenta are $k_\pm = k \pm P/2$. Ball and Chiu suggested to separate the vertex into the transverse parts $V_\mu^{(5,\dots,8)}$ with $P_\mu V_\mu^{(5,\dots,8)} = 0$ and four non-transverse components $V_\mu^{(1,\dots,4)}$. The latter ones are completely fixed in terms of the quark dressing functions $M(p^2)$ and $Z_f(p^2)$ by the WTIs and the demand of regularity [23]. This part of the quark–photon vertex is also called the Ball–Chiu- or BC-vertex.

The additional eight components of the transverse part are determined numerically through a self-consistent solution of the BSE, Fig. 4. It is an important property of this equation that it generates dynamically vector meson bound-state poles. The idea of vector meson dominance then corresponds to the suggestion that the transverse part of the quark–photon vertex provides the leading contributions in a calculation at hand. While this is indeed correct for some observables, as for example for a_μ^{HVP} below, other examples are known where this idea is not correct and sizable contributions from the BC-part of the vertex occur, see e.g. [24].

3.3. The hadronic vacuum polarisation

Finally we give some details regarding the calculation of the hadronic vacuum polarisation. Within the truncation scheme proposed above, the hadronic tensor is given by

$$\Pi_{\mu\nu}(P) = Z_2 \int_q \mathrm{tr}\big[S(q_-) \Gamma_\mu(P, q) S(q_+) \gamma_\nu \big], \qquad (15)$$

where $q_\pm = q \pm P/2$ and Z_2 is the quark wave function renormalisation. The scalar function $\Pi(P^2)$ is obtained via Eq. (7). This quantity is logarithmically divergent and so requires renormalisation. We apply the condition $\Pi_R(0) = 0$ through the subtraction

$$\Pi_R(P^2) := \Pi(P^2) - \Pi(0), \qquad (16)$$

which effectively amounts to adjusting the constant Z_3 in Eq. (4) appropriately. In addition we need to take care of quadratic divergences that appear through our use of a hard numerical cutoff. These can be subtracted at $p^2 = 0$ or projected out using the method of Brown and Pennington [25]. Both procedures agree very well.

To check our numerics, we first evaluated the perturbative QED one-loop result (see e.g [26]) and found excellent agreement. In particular we checked that the calculation of Π_R was independent
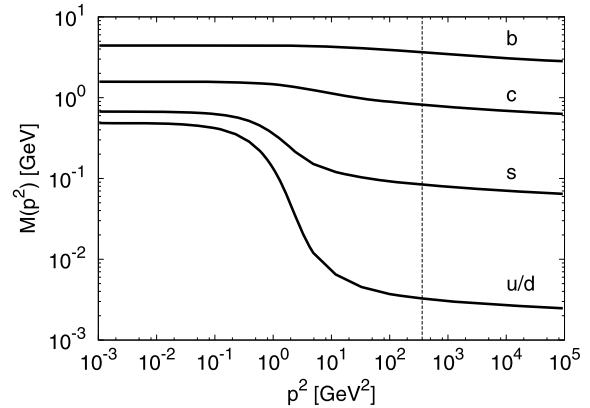

Fig. 5. The quark mass functions of the u/d, s, c and b quarks obtained from the quark DSE. The dashed vertical line represents the renormalisation point $\mu^2 = (19 \ \mathrm{GeV})^2$.

of the cut-off. As a further check, we evaluated the electron loop contribution to a_μ via Eq. (8) by replacing the propagator and vertices with their tree-level values. We reproduced the well-known result $a_\mu^{\mathrm{vac.pol.,e\text{-}loop}} \approx 5.904 \times 10^{-6}$ [1] on the sub permille level. For our general calculations with dressed momentum dependent quark propagator and quark–photon vertex we estimate a numerical error of roughly two to three percent due to the uncertainties related with the renormalisation procedure discussed above.

Below we present the results of our calculation for the Adler function as well as the anomalous magnetic moment of the muon a_μ. We use the Maris–Tandy interaction with the two different parameter sets discussed above. We solve the quark DSE, Fig. 3, for five quark flavors u, d, s, c and b, and work in the isospin symmetric limit $m_u = m_d$. The resulting quark mass functions are shown in Fig. 5. They dynamically connect the infrared constituent quark mass region with the ultraviolet current quark mass region and thus provide a unified approach to both pictures. Note that our quark agrees qualitatively with lattice calculations [27].

Once the quarks are obtained we solve for the quark–photon vertex, Eq. (13). Here, no additional approximations are made, *i.e.* we take into account all twelve tensor structures and the full momentum dependence of the vertex. This is done for each flavor separately and hence we can calculate $\Pi_{\mu\nu}$ using Eq. (15) which sums over all quark flavors. With $\Pi_{\mu\nu}$ at hand we can obtain the hadronic contribution to the anomalous magnetic moment of the muon via Eq. (8), and the Adler function from Eq. (9).

Let us emphasise again that contributions from the vector meson sector are generated dynamically in our approach. For the light meson sector this means that adding up contributions from the up, down and strange quarks we automatically take into account contributions from the ρ, ω and ϕ meson resonant parts. Since we are working in the isospin limit, the ρ and ω meson contributions are degenerate whereas the contribution of the ϕ is pure $s\bar{s}$. We also do not take into account electromagnetic mixing effects. These will be explored in future work.

4. Results

In Fig. 6 we show our result for the Adler function as calculated using parameter set II of Table 1, together with the result from dispersion relations [1,4]. The Dyson–Schwinger solution describes the data very well in the non-perturbative region $Q < 1$ GeV. We also see that in the asymptotic ultraviolet limit the solution follows the result from the dispersion relations. The differences between set I (not shown) are limited to the slope of the function
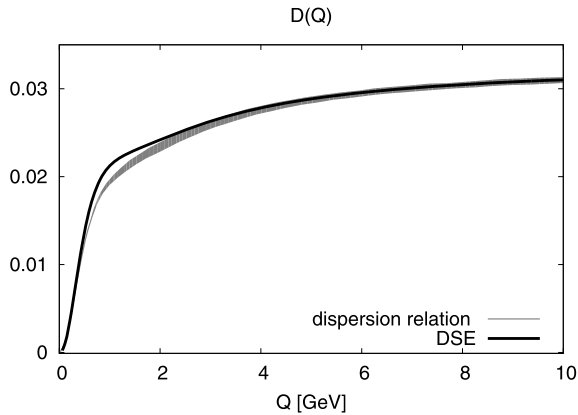
Fig. 6. The Adler function obtained from DSE's for the Maris–Tandy model together with the dispersion relation results from [28,4].
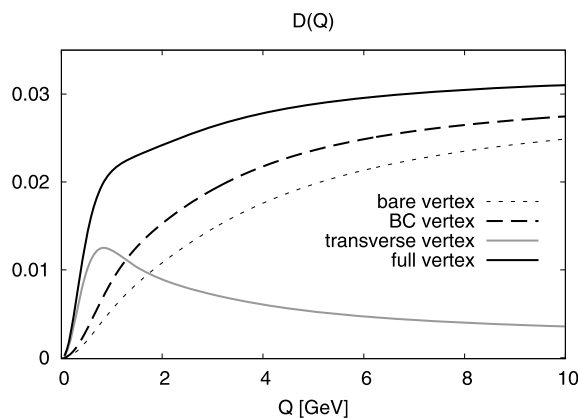

Fig. 7. The Adler function obtained in the MT model defined in Eq. (12) via Eq. (15) with different vertex dressings.

Table 2
The leading-order HVP contribution to a_μ as obtained by our two sets of bare quark masses for different truncations of the quark–photon vertex.

$a_\mu^{HVP} \times 10^{11}$	Bare	BC	Transverse	Full
Set I	760	1280	6160	7440
Set II	720	1120	5640	6760

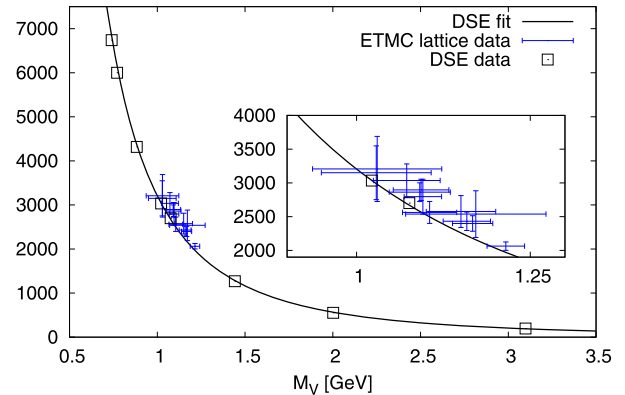**Fig. 8.** The mass dependence of $a_\mu^{HVP} \times 10^{11}$, for two flavours, plotted wrt the mass of the light vector meson. Shown is the data from this work (DSE) together with a fit ($a_\mu \propto M_V^{(-2.5)}$). In addition we show recent data from the ETMC lattice collaboration [15].

thus be excited from the vacuum too easily. This, however, is already a reassuringly good result for a calculation performed with standard parameters without adjustment. Changing our input mass parameters to values that are matched to the vector meson sector improves our value for a_μ^{HVP} such that deviations with experiment fall below three percent. We regard this agreement as a clear signal that our approach accurately contains the physics relevant for the hadronic contributions to a_μ, which entails that indeed the dynamics associated with the vector meson pole, together with gauge invariance, are the two essential ingredients.

Next we examine the dependence of a_μ^{HVP} on the quark–photon vertex used in Eq. (15). The results can be found in Table 2. As expected from our results for the Adler function, most of the contribution to a_μ^{HVP} comes from the transverse parts of the vertex containing the vector meson poles. Here also most of the differences between our parameter sets I and II occur. However, there are also sizable contributions from the gauge or Ball–Chiu part of the vertex and only the use of the full vertex gives satisfying results for a_μ^{HVP}. Once more, this emphasises the interplay of contributions related to resonances and those demanded by gauge symmetry.

Finally we look closer at the dependence of a_μ^{HVP} on the quark mass. This behaviour is conveniently parametrised by plotting against a scheme independent, physical mass such as for example the pseudoscalar or vector meson mass m_V. Both of these can be determined in our approach via a solution of their corresponding Bethe–Salpeter equations. In Fig. 8 we show our results for $a_\mu^{HVP}(m_V)$ compared to a recent lattice study of the ETMC-Collaboration [15]. Overall we find very good agreement between the two approaches, with our values inside their error bars. The same level of agreement is seen between our calculation and the new lattice determination for $N_f = 2 + 1$ flavour QCD presented in Ref. [29].

5. Discussion

Our results for a_μ^{HVP} clearly show the importance of dressing effects in the quark–photon vertex. Here, particularly rele-

in the low momentum region, which is most sensitive to the mass of the vector meson (see Fig. 7). Note in addition that most of the contributions to a_μ^{HVP} come from the region around the muon mass and that the integration of Eq. (8) saturates between 0.5 and 1 GeV. From the Adler function we therefore expect similar results for a_μ^{HVP} for both parameter sets with small deviations on the level of ten percent.

Before we discuss our results for a_μ^{HVP} we take a closer look at the impact of the transverse parts of the quark–photon vertex as compared to its non-transverse Ball–Chiu (BC) structure. In Fig. 7 we compare the full results with the one using the BC-part alone or even neglecting all vertex dressing altogether.

Clearly, the bare and Ball–Chiu vertices do not provide sufficient contributions to the Adler function, yielding functions that are only half the height of the full vertex result in the infrared. Only the full vertex calculated from its inhomogeneous Bethe–Salpeter equation contains vector meson poles dynamically in its transverse structure. Obviously these are essential to describe the data correctly.

This sensitivity to the vector meson sector is especially seen in a_μ^{HVP}. For the two mass parameter sets I, II of our model and the full quark–photon vertex we find

$$a_\mu^{HVP,I} = 7440 \times 10^{-11}, \tag{17}$$

$$a_\mu^{HVP,II} = 6760 \times 10^{-11}. \tag{18}$$

As expected, our first mass parameter set yields a value for a_μ^{HVP} which is too large by about eight percent, due to the fact that our vector meson for this parameter set is slightly too light and can

vant are its dynamically generated vector meson poles in the transverse part of the vertex. However, we wish to emphasise again that this importance crucially depends on the kinematic and dynamical details of the problem at hand. For example, the transverse parts of the vertex contribute towards only half of the pion charge radius [20], whilst in the pion pole approximation of the light by light contributions to *g*-2 they constitute only a thirty percent effect as compared to the BC-part [8,9].

It is thus very dangerous to transport expectations based on one process blindly to another; explicit calculations should always be preferred. In this work, we have performed such a calculation for a_μ^{HVP} by including both the BC- and transverse parts of the vertex explicitly. For a_μ^{LBL} in Refs. [8,9], the algebraic complexity forced us to consider initially only the BC-part of the vertex, with transverse parts estimated from other model calculations. Preliminary results for a_μ^{LBL} with the full vertex have been presented at [30], and show that gauge effects still dominate. The details of this will be presented in a future work.

We also wish to discuss the arguments made in Ref. [16]. There, a constituent quark model with momentum independent masses has been combined with a perturbative evaluation of gluonic corrections. Corresponding results for a_μ^{HVP} and a_μ^{LBL} have been compared. The authors point out that neglecting radiative corrections, they need unphysically small constituent quarks masses to reproduce the experimental value for a_μ^{HVP}. From our results we can see clearly that this is merely the result of compensating for dynamics that are absent in the quark–photon interaction of that model. The authors take note of that fact and argue that this very light constituent quark mass effectively includes the $\gamma - \rho$-coupling g_ρ via $M_q \propto M_\rho/g_\rho$. This simple relation might however be inappropriate for very dissimilar kinematics. In addition the authors of Ref. [16] find very large corrections when they include radiative corrections on the one-loop level. They observed that these corrections could be absorbed into a change of the constituent quark mass with stable results for a_μ^{HVP} and a_μ^{LBL}. Based on this result the authors suggest that dressing effects in the quark–photon vertex of the full theory should be small. We disagree with this conclusion. First of all, it is dangerous to interpret a truncated perturbative expansion that features both a large expansion parameter and large expansion coefficients. Second, non-perturbative features such as the formation of bound-states (as generated dynamically by the vertex) are absent in their calculation. Thus we take their results as a hint that (infinitely many) higher contributions are important and should be included as consistently as possible, since any finite order pQCD cannot give satisfactory answers.

We have done exactly this in our calculation. As a result we found that the leading-order contribution comes from vector meson (VM) poles accounting for roughly 80% of a_μ^{HVP}, with the remainder coming from corrections induced by gauge invariance. The dynamics of the VM poles are thus important but not the whole story. This tells us that an effective model that features only VM exchange should be a good approximation, but will miss out on other important contributions that cannot be integrated by reshuffling of contributions. Similarly, a constituent quark loop approach would not contain any dynamical degrees of freedom relating to vector meson exchange. This is in contradiction to what is observed both on the lattice and in our Dyson–Schwinger calculation, and thus the constituent quark model cannot be a satisfactory description of the process at hand.

Finally, we believe that the good agreement of our results for a_μ^{HVP} with experiment *and* with lattice calculations adds credit to our corresponding approach to a_μ^{LBL}.

6. Summary

We calculated the hadronic vacuum polarisation using the method of Dyson–Schwinger equations, taking into account the five lightest quark flavors. As input we used a phenomenologically successful model for the quark–gluon interaction together with the rainbow-ladder truncation. The parameters of these interactions as well as the quark masses were fixed by meson observables such as masses and decay constants, without additional fine-tuning. We determined the quark–photon vertex from its inhomogeneous Bethe–Salpeter equation in the same approximation and subsequently calculated the hadronic vacuum polarisation tensor. From these we obtained results for the anomalous magnetic moment of the muon $a_\mu^{HVP,LO}$ as well as for the Adler function. Both quantities agree well with model independent results extracted from experiment. In particular, the Adler function is reproduced very well in the strictly non-perturbative region at small momenta. We have shown that one requires a description in terms of dynamical quarks interacting through non-perturbative gluons in order to achieve this level of accuracy.

Consequently we find results for the muon anomaly in good agreement with other determinations. Our best result using the quark mass parameter set II is

$$a_\mu^{HVP,LO} = 6760 \times 10^{-11}. \tag{19}$$

This can be compared to the leading-order result quoted in Eq. (3), $6903.0(52.6) \times 10^{-11}$. The difference is at the level of two percent. A comparison with the result $a_\mu^{HVP,LO} = 7440 \times 10^{-11}$ obtained with our parameter set I may serve as an estimate for the systematic uncertainty of our model of roughly ten percent. We believe our approach to the hadronic light-by-light scattering contribution [8,9], which employs the same truncation scheme, will ultimately lead to results with similar precision. However, note that in Ref. [8,9] the full quark–photon vertex was not yet included in the quark loop due to its algebraic complexity. Improvements along this direction are underway.

References

[1] F. Jegerlehner, A. Nyffeler, Phys. Rep. 477 (2009) 1, arXiv:0902.3360 [hep-ph].
[2] G.W. Bennett, et al., Muon G-2 Collaboration, Phys. Rev. D 73 (2006) 072003, arXiv:hep-ex/0602035.
[3] B.L. Roberts, Chin. Phys. C 34 (2010) 741, arXiv:1001.2898 [hep-ex].
[4] F. Jegerlehner, The Anomalous Magnetic Moment of the Muon, Springer Tracts in Modern Physics, vol. 226, Springer, Berlin, Germany, 2008, 426 pp.
[5] M. Davier, A. Hoecker, B. Malaescu, et al., Eur. Phys. J. C 71 (2011) 1515, arXiv:1010.4180 [hep-ph].
[6] K. Hagiwara, R. Liao, A.D. Martin, D. Nomura, T. Teubner, arXiv:1105.3149 [hep-ph].
[7] M. Benayoun, P. David, L. DelBuono, F. Jegerlehner, arXiv:1106.1315 [hep-ph].
[8] C.S. Fischer, T. Goecke, R. Williams, Eur. Phys. J. A 47 (2011) 28, arXiv:1009.5297 [hep-ph].
[9] T. Goecke, C.S. Fischer, R. Williams, Phys. Rev. D 83 (2011) 094006, arXiv:1012.3886 [hep-ph].
[10] E. de Rafael, Phys. Lett. B 322 (1994) 239, arXiv:hep-ph/9311316.

[11] E. Pallante, Phys. Lett. B 341 (1994) 221, hep-ph/9408231.
[12] J.S. Bell, E. de Rafael, Nucl. Phys. B 11 (1969) 611.
[13] A.E. Dorokhov, Phys. Rev. D 70 (2004) 094011, hep-ph/0405153.
[14] M. Della Morte, B. Jager, A. Juttner, H. Wittig, AIP Conf. Proc. 1343 (2011) 337, arXiv:1011.5793 [hep-lat].
[15] X. Feng, K. Jansen, M. Petschlies, D.B. Renner, arXiv:1103.4818 [hep-lat].
[16] R. Boughezal, K. Melnikov, arXiv:1104.4510 [hep-ph].
[17] P. Maris, P.C. Tandy, Phys. Rev. C 60 (1999) 055214.
[18] P. Maris, C.D. Roberts, Int. J. Mod. Phys. E 12 (2003) 297, nucl-th/0301049.
[19] C.S. Fischer, J. Phys. G 32 (2006) R253, hep-ph/0605173.
[20] P. Maris, P.C. Tandy, Phys. Rev. C 61 (2000) 045202, arXiv:nucl-th/9910033.
[21] M.S. Bhagwat, P. Maris, Phys. Rev. C 77 (2008) 025203.

[22] P. Maris, AIP Conf. Proc. 892 (2007) 65.
[23] J.S. Ball, T.W. Chiu, Phys. Rev. D 22 (1980) 2542.
[24] P. Maris, P.C. Tandy, Nucl. Phys. A 663 (2000) 401.
[25] N. Brown, M.R. Pennington, Phys. Rev. D 39 (1989) 2723.
[26] V.P. Nair, Quantum Field Theory: A Modern Perspective, Graduate Texts in Contemporary Physics, Springer, New York, USA, 2005, 557 pp.
[27] P.O. Bowman, U.M. Heller, D.B. Leinweber, M.B. Parappilly, A.G. Williams, J.b. Zhang, Phys. Rev. D 71 (2005) 054507, arXiv:hep-lat/0501019.
[28] S. Eidelman, F. Jegerlehner, A.L. Kataev, O. Veretin, Phys. Lett. B 454 (1999) 369.
[29] P. Boyle, L. Del Debbio, E. Kerrane, J. Zanotti, arXiv:1107.1497 [hep-lat].
[30] R. Williams, talk at the Workshop on the hadronic light-by-light scattering contribution to the muon magnetic anomaly, INT, Seattle 02/28–03/04, 2011.